

# Infiltration of Outdoor Ultrafine Particles into a Test House

Donghyun Rim  
Lance Wallace  
Andrew Persily

Indoor Air Quality and Ventilation Group, Energy and Environment Division  
Engineering Laboratory, National Institute of Standards and Technology  
100 Bureau Drive Gaithersburg, MD 20899

Content submitted to and published by:  
Environmental Science and Technology  
2010; Volume 44: 5908-5913

U.S. Department of Commerce  
*Dr. Rebecca M. Blank, Acting Secretary*



National Institute of Standards and Technology  
*Patrick D. Gallagher, Director*

## DISCLAIMERS

Certain commercial entities, equipment, or materials may be identified in this document in order to describe an experimental procedure or concept adequately. Such identification is not intended to imply recommendation or endorsement by the National Institute of Standards and Technology, nor is it intended to imply that the entities, materials, or equipment are necessarily the best available for the purpose.

Any link(s) to website(s) in this document have been provided because they may have information of interest to our readers. NIST does not necessarily endorse the views expressed or the facts presented on these sites. Further, NIST does not endorse any commercial products that may be advertised or available on these sites.

# Infiltration of Outdoor Ultrafine Particles into a Test House

Donghyun Rim, Lance Wallace, Andrew Persily

## Abstract

Ultrafine particles (UFP) ( $< 100$  nm) have been related to adverse human health effects such as oxidative stress and cardiovascular mortality. However, human exposure to particles of outdoor origin is heavily dependent on their infiltration into homes. The infiltration factor ( $F_{inf}$ ) and its variation as a function of several factors becomes of enormous importance in epidemiological studies. The objective of this study is to investigate the transport of UFP into a residential building and to determine the functional dependence of infiltration on particle size and air change rate. A secondary objective was to estimate the values of the penetration coefficient  $P$  and composite deposition rate  $k_{comp}$  that enter into the definition of  $F_{inf}$ . Using continuous measurements of indoor and outdoor concentrations of size-resolved particles ranging from 5 nm to 100 nm in a manufactured test house, particle penetration through the building, composite deposition, and the resulting value of  $F_{inf}$  were calculated for two cases: closed windows and one window open 7.5 cm.  $F_{inf}$  ranged from close to 0 (particles  $< 10$  nm) to 0.3 (particles  $> 80$  nm) with windows closed and from 0 to 0.6 with one window open. The penetration coefficient (closed windows) increased from about 0.2 for 10-nm particles to an asymptote near 0.6 for particles from 30-100 nm. Open window penetration coefficients were higher, ranging from 0.6 to 0.8. Closed-window composite deposition rates, which included losses to the furnace filter and to the ductwork as well as to interior surfaces, monotonically decreased from levels of about  $1.5 \text{ h}^{-1}$  for 10-nm particles to  $0.3 \text{ h}^{-1}$  for 100-nm particles. For the open-window case, composite deposition rates were higher for particles  $< 20$  nm, reaching values of  $3.5 \text{ h}^{-1}$ . Mean standard errors associated with estimates of  $P$ ,  $k_{comp}$ , and  $F_{inf}$  for two series of measurements ranged from 1.0% to 4.4%.

**Keywords:** ultrafine particles; infiltration; deposition; penetration; dynamic modeling

## **Introduction**

During the past decade, epidemiological studies have demonstrated that outdoor particles are associated with adverse human health outcomes (1, 2), particularly respiratory and cardiovascular diseases. Ultrafine particles (UFP), which are smaller than 100 nm in diameter, may be more important in inhalation exposure than  $PM_{2.5}$  ( $< 2.5\mu m$ ) or  $PM_{10}$  ( $< 10\mu m$ ) (3, 4). The large relative surface area of UFP can make toxic air pollutants such as polycyclic aromatic hydrocarbon (PAH) and transition metals more biologically available (5, 6). UFP inhaled by human beings are suspected to induce pulmonary inflammation and enter the blood circulation, damaging other sites in the cardiovascular system (5, 7). They have also been shown to induce oxidative-stress alterations of DNA in humans following 24-h exposure to vehicle emissions (8) and have been implicated in human mortality (3).

Two main sources of outdoor UFP are primary combustion products from automobile exhaust (9) and photochemical reactions in the atmosphere (10). Indoor UFP sources include electric and gas stoves (11, 12, 13), vented gas clothes dryers (14), and electric motors (15). Also, chemical reactions between terpene and ozone indoors produce UFP as byproducts (16, 17). People spend most of their time indoors (18) and outdoor particles can penetrate through the building envelope. Therefore, human exposure to UFP in buildings depends on both outdoor and indoor sources.

UFP penetrate into the house by air infiltration (uncontrolled airflow through leakage paths in the building envelope) or through open windows. The particle penetration efficiency is a function of building crack characteristics, indoor-outdoor pressure difference, and particle size (19, 20, 21). Factors influencing particle deposition include particle size, building ventilation

characteristics, indoor air speed, turbulence intensity, room geometry and the orientation and roughness of the deposition surface (21, 22, 23).

The fraction of the ambient particles that penetrates indoors and remains suspended under steady-state conditions is defined as the infiltration factor ( $F_{inf}$ ) (24, 25). Variability of  $F_{inf}$  within and across homes is enormously important in determining the fraction of total exposure due to outdoor air particles. Epidemiological studies that estimate the effect of outdoor air particles on public health almost exclusively rely on outdoor measurements at central monitoring sites. These studies assume that the monitored outdoor concentrations represent (to within a constant factor) personal exposures of the entire population in the area, even though the magnitudes of the infiltration factors can vary by up to a factor of 3 across homes (26). A poor correlation between outdoor particle concentration and personal exposure to particles of outdoor origin can result in a poor estimate of the associated health effect.

For a given building under steady-state conditions,  $F_{inf}$  is a function of particle penetration efficiency ( $P$ ), air change rate ( $a$ ), and composite deposition rate ( $k_{comp}$ ):

$$F_{inf} = \frac{Pa}{a + k_{comp}} \quad (1)$$

In this equation, the composite deposition rate  $k_{comp}$  is a composite of at least three processes: deposition to interior surfaces in the conditioned area; capture on the furnace filter; and deposition to ductwork when the central fan is on. In our studies, a central air conditioning unit was always on, and therefore all three processes were active at all times.

Note that  $P$  is dimensionless and lies between 0 and 1,  $a$  and  $k_{comp}$  have the same dimension (inverse time), and therefore the infiltration factor is a dimensionless fraction between 0 and  $P$ . The values of  $P$  and  $k_{comp}$  depend strongly on particle size.

Several previous studies have evaluated infiltration factors (13, 24-28). Hoek et al. (27) measured particle number concentrations (7 nm to 3  $\mu\text{m}$ ) outside and inside homes in four European cities. The study observed infiltration factors ranging from 0.06 to 0.43. Long et al. (13) reported infiltration factors for nine Boston homes ranging from 0.2 to close to 1 for particles sized between 20 nm and 100 nm.

The present study investigates the infiltration, penetration, and deposition of size-resolved UFP, including the seldom-studied diameters  $< 10$  nm. The results from the measurements and analytical modeling of the present study can be used to improve prediction of occupant exposure to UFP.

## **Methods**

### *Test House description*

The experimental measurements were conducted in a manufactured test house. The house consists of three bedrooms, two baths, kitchen, family room, and dining and living area, having a floor area of 140  $\text{m}^2$  and a volume of 340  $\text{m}^3$  (see the floor plan in the Supporting Information, Figure S1).

### *Measurements of air change rate and UFP concentrations*

Air change rate and size-resolved particles in the test house were monitored on 19 weekends from August 2008 to September 2009. During the weekend measurements, the house was uninhabited. Air change rates were measured using a tracer gas ( $\text{SF}_6$ ) decay technique. The tracer gas was released into the living room at 4-hr intervals using an automated system and the decaying concentrations were monitored at 10-minute intervals at six locations in the house

(master bedroom, bedroom 2, living room, family room, dining room, and kitchen). The concentrations were measured using gas chromatography with electron capture detection (GC/ECD), and the air change rate was estimated by regressing the natural logarithm of the tracer gas concentration versus time (29). Following the injection of the tracer gas, it normally took about one hour for all rooms to be well-mixed, with relative standard deviations (RSDs) <0.1. Moving-average 70-minute regressions were then calculated to determine air change rates. The majority of RSD values were <0.1.

Along with the air change rate, measurements of size-resolved particles were performed indoors and outdoors using a scanning mobility particle sizer (SMPS) (Model 3936, TSI, St. Paul, MN). The SMPS consists of an electrostatic classifier (Model 3080), a nano-differential mobility analyzer (Nano-DMA, Model 3085) and a water-based condensation particle counter (CPC; Model 3786). The SMPS monitored particles ranging from 2 nm to 64 nm using a sheath flow rate of 15 L/s and an aerosol flow rate of 1.5 L/s (10:1 sheath/aerosol flow ratio). About half the time, the SMPS monitored particles from 3 nm to 100 nm using a sheath flow rate of 6 L/s and an aerosol flow rate of 0.6 L/s. The larger flow rates were achieved by adding a bypass pump (Model 3032, TSI) with a critical flow orifice (Model W-13-SS, O'Keefe, Trumbull, CT) to the system. Therefore, the measurements with the SMPS were capable of providing real-time particle number concentration and size distribution in the range from 2 nm to 100 nm.

The SMPS was located in the master bedroom (Figure S1) and monitored size-resolved UFP inside and directly outside the house. The sampling rate of UFP was set at 2.5 min: 2 min of measurement and 30 s for the voltage to return to baseline. An automatic switching system was used to allow monitoring indoors and outdoors sequentially. The valve in the system could directly switch between sampling between indoor air and outdoor air according to the timing

circuit. Using the switching system, indoor and outdoor UFP concentrations were alternately measured with an interval of 5 min to 10 min (2 to 4 consecutive scans for each location). Nine experiments were with closed windows, and 10 with a single window open about 7.5 cm. Each experiment lasted about 60 hours, typically from 3 PM on a Friday to 9 AM on the following Monday. Nominally about 1440 UFP measurements were thus available, 720 in outdoor air and 720 in indoor air.

### *Data Analysis*

In the absence of indoor sources, the main factors determining the indoor UFP concentrations are the penetration through the building envelope of outdoor UFP, deposition of particles on indoor surfaces, and air change rate. Incorporating these three factors into a mass-conservation model and considering the indoor volume acting as a well-mixed reactor, the dynamic indoor particle concentration can be written as follows:

$$\frac{dC_{in}}{dt} = PaC_{out} - (a + k_{comp})C_{in} \quad (2)$$

Recirculated air at approximately 5 house volumes per hour went through the central furnace filter and ductwork. The result is increased particle deposition on the filter and ductwork surfaces (30). However, other losses such as particle coagulation are expected to be relatively small, given that the ultrafine particle concentrations in the house were generally lower than  $5,000 \text{ cm}^{-3}$  in most of the measurements

Equation (2) is valid for particles of all sizes, but will have different values of  $P$  and  $k_{comp}$  for each size. The 97 particle size bins ranging from 2 nm to 64 nm or from 3 nm to 100 nm were categorized in groups of 5 adjacent particle size bins, with each bin containing the sum of the

five number concentrations. Equation (2) was then applied to each category, identified by the geometric mean diameter of the 5 size ranges. At each discrete time step, assuming constant  $P$  and  $k_{comp}$ , the predicted indoor particle concentration at time  $t$  ( $C_{in,t}$ ) was calculated for each particle size category using the difference form of Equation (2):

$$C_{in,t} = Pa_t C_{out,t} \Delta t + (1 - (a_t + k_{comp}) \Delta t) C_{in,t-1} \quad (3)$$

where  $a_t$  is the air change rate and  $C_{out}$  is the outdoor concentration at time  $t$ , and  $\Delta t$  is the time step (in this case 2.5 minutes). This relatively small time step (0.04 h) allowed approximating the exponential decay of the indoor concentration by the linear term in Equation (3).

Comparing the calculated and measured concentration profiles over a 60-hour period, the best-fitting values of the penetration coefficient  $P$  and composite deposition rate  $k_{comp}$  were determined by minimizing the sum of the absolute differences between the modeled and observed indoor number concentrations, using the Excel Solver function. No effort was made to constrain the ranges of  $P$  or  $k_{comp}$ , such as requiring  $P < 1$  or  $k_{comp} > 0$ . The best estimates of  $P$  and  $k_{comp}$  were then combined with the average air change rate over the experimental period to estimate the infiltration factor for a given particle size category. An independent check on  $F_{inf}$  was provided by the mean indoor/outdoor ratio, assuming no indoor sources during the entire weekend. The mean was calculated without the first 120 values (5 hours) in case experiments on Friday morning may have affected the beginning of the indoor-outdoor measurements Friday afternoon. Because the outdoor values were available only half of the time, the missing outdoor values were linearly interpolated so that the model could predict an indoor value for these times. The missing indoor values were not interpolated, since there was no need; thus only observed indoor values were compared to those predicted by the model. This provided a nominal number

of 720 paired indoor measurements and model predictions for each experiment. To avoid influencing the results by the choice of a starting point for the indoor concentration, the first 120 values (5 hours) were not counted in the sum of absolute differences. (The choice of 5 hours was made after testing to see that whether choosing 0 or 1000 for the initial value of  $C_{in}$  did not affect the model estimate after 3-4 hours.) This procedure provided  $P$  and  $k_{comp}$  estimates for about 18 size categories. Using these estimates of  $P$  and  $k_{comp}$ , the predicted indoor air concentrations were compared to the measured values by linear regression. If the resulting  $R^2$  value was  $>90\%$ , the estimates of  $P$  and  $k$  were accepted as valid. 196 of the 342 possible estimates exceeded a  $90\% R^2$  value. Most of the cases not achieving high  $R^2$  values were associated with the smallest particles, which are scavenged in outdoor air as particles age and which, even if present in outdoor air, have difficulty penetrating the building envelope and remaining suspended for long periods. To calculate the uncertainty associated with the estimates of  $P$  and  $k_{comp}$ , a Visual Basic macro called Solver Aid was employed (32). This program returns an estimate of the standard error for each parameter whose point estimates are provided by Solver. The program has been tested on sample data against commercial software such as NLIN from SAS and has been shown to give identical uncertainty estimates (33). Since the program assumes minimization of the sum of squared errors, whereas our initial approach chose minimization of the sum of absolute differences between observed and predicted values, we recalculated the estimates of  $P$  and  $k_{comp}$  using the sum of squared errors for two sets of measurements including both a closed window and open window case. This allowed not only the formal determination of the standard error associated with the Solver estimates of  $P$  and  $k_{comp}$ , but also an indication of the effect of choosing a different function (squared errors vs absolute differences) for minimization.

The functional dependence of  $F_{inf}$  on particle size and measured air change rate was investigated using multiple linear regression analysis. Before doing the regression, dependencies among all the variables were tested; air change rate and window position were collinear. Therefore, the window position variable was dropped in the regression analysis, using the criterion of the least important parameter.

## **Results and Discussion**

### *Calculation of uncertainty*

Because of the difficulty in calculating  $P$  and  $k$  encountered by other researchers (13, 24, 34), the uncertainty of the determination was scrutinized by several approaches. First, estimates of the standard errors returned by the Solver Aid program were calculated for two of the experiments—one with closed windows and one with one window open 7.5 cm (Table 1). Individual estimates of uncertainty for  $P$  and  $k_{comp}$  ranged from 0.4% to 5.0% with mean errors ranging from 1.0% to 2.4%. These errors were propagated in quadrature to estimate the error in  $F_{inf}$ . Individual errors for  $F_{inf}$  ranged from 0.8% to 6.5% and the mean error was 1.7% for the closed window case and 2.4% for the open window case.

Uncertainty in the  $F_{inf}$  estimate was characterized by comparing the estimated value using the best values of  $P$  and  $k_{comp}$  to the measured I/O ratios for the same two open window and closed windows cases (Table 2). Agreement was very good.

Other estimates of uncertainty included varying  $k_{comp}$  by nominal 10% amounts and varying  $P$  to keep the same value of  $F_{inf}$ , followed by calculating the increase in the sum of squared errors. This increase was then compared to the formal estimate of the standard deviation of this sum. The increase was always much larger than the formal standard deviation, indicating

the stability of the  $P$  and  $k_{comp}$  estimates. These uncertainty approaches are discussed further in Supporting Information.

The effect of minimizing the sum of squared errors vs. absolute differences is shown in Table S1 (Supporting Information). The mean differences in estimates of  $P$ ,  $k_{comp}$ , and  $F_{inf}$  ranged from 1.3% to 4.4%.

### *Air change rate*

An example of measured air change rates is described in Figure S2 in the Supporting Information. For all the study periods, the 3-day average air change rate ranged from 0.14 h<sup>-1</sup> to 0.44 h<sup>-1</sup> with all windows closed and from 0.18 h<sup>-1</sup> to 0.63 h<sup>-1</sup> with one window open by 7.5 cm. Rates with one window open (mean 0.41 h<sup>-1</sup>, SD 0.13 h<sup>-1</sup>) were higher than those with all windows closed (mean 0.25 h<sup>-1</sup>, SD 0.10 h<sup>-1</sup>).

### *Infiltration factors*

Figure 1 compares the measured and predicted concentrations for one size category (22 nm to 26 nm) during one open window experiment (October 17-20, 2008). The penetration coefficient  $P$  and composite deposition rate  $k_{comp}$  that predicted the measured (time-varying) concentrations with the smallest error were calculated as 0.823 (95% CI 0.814-0.833) and 1.05 (1.03-1.07) h<sup>-1</sup>, respectively. The resulting infiltration factor  $F_{inf}$  was 0.307 (0.284-0.329). Figure 2 presents the regression analysis between the measured and modeled concentrations. Since the  $R^2$  value for the regression is 0.994, the estimates for  $P$ ,  $k_{comp}$ , and  $F_{inf}$  were considered valid.

Size-resolved infiltration factors as a function of particle diameter were estimated for the 9 weekend measurements with all windows closed (Figure 3a). The infiltration factor increases with particle size and air change rate. For UFP, Brownian and turbulent diffusion are more important factors for particle losses in buildings and cracks, compared to impaction or gravitational settling (35). Figure 3a shows that the infiltration factor generally increases with air change rate. The size-resolved infiltration factors observed with one window open are shown in Figure 3b. The infiltration factor ranged between 0 and 0.5, larger than for closed windows.

The trend of increasing infiltration factor with particle diameter agrees with the study by Zhu et al. (36) that reported an infiltration factor range from 0.1 to 0.4 for small UFP (10 nm to 20 nm) in the cases of closed and open windows, while the factor ranged from 0.6 to 0.9 for larger UFP (70 nm to 100 nm). Long et al. (13) also found that the mean infiltration factor for the nine homes studied was 0.49 for 20-nm particles and increased up to 0.73 for 100 nm particles.

#### *Penetration coefficient*

Figure 4a indicates that the penetration coefficients increase from about 0.2 at the smallest sizes to an asymptote of about 0.55 for the closed-window case, and from higher levels of about 0.6 to an asymptote of 0.75 for the open window case. The open window case allowed estimates of penetration coefficients for two or three smaller size categories than were possible in the closed window case. The comparison of the estimates with a theoretical model (22) is described in Supporting Information.

## *Deposition*

Figure 4b shows that the composite deposition rates were similar for the open and closed window cases for particles  $> 20$  nm, but diverged for particles  $< 20$ nm, with the rate for the open window case reaching twice that for the closed window case at the smaller diameters.

For particles smaller than 30 nm, the composite deposition rates ( $1 \text{ h}^{-1}$  to  $3.5 \text{ h}^{-1}$ ) were much higher than the air change rates ( $0.1$  to  $0.6 \text{ h}^{-1}$ ). This result suggests that for smaller UFP the loss due to deposition is substantially higher than that due to air change rate in residential houses with central forced air and extensive use of the furnace fan.

The strong dependence of particle deposition on particle size observed in the present study agrees with those in previous studies in literature (13, 21, 23, 31, 37-38). Wallace et al. (38) found that UFP deposition rates decrease from  $6.0 \text{ h}^{-1}$  for 10 nm particles to  $0.1 \text{ h}^{-1}$  for 100-nm particles depending on particle size and loss mechanisms associated with usage of air-circulation fan and in-duct filters. Other studies (13, 21, 23, 31) also reported from experiments in real rooms and chambers that deposition rates for UFP (10 nm to 100 nm ) increase from  $0.05 \text{ h}^{-1}$  up to  $6.0 \text{ h}^{-1}$  as particle size decreases.

A multiple linear regression of  $F_{inf}$  on air change rate and particle size explained 80% of the observed variance (N = 291 observations). The intercept was 0.107 (SE 0.009) and the coefficients for the particle diameter (nm) and air change rate ( $\text{h}^{-1}$ ) were 0.0034 (SE 0.0001;  $p < 0.0001$ ) and 0.45 (SE 0.02;  $p < 0.0001$ ), respectively.

Previous studies (13, 24-25, 34) have reported very broad confidence intervals around their estimates of  $P$  and  $k_{comp}$ . In this study, we have achieved quite tight bounds on our estimates of  $P$  and  $k_{comp}$ . There were several aspects of our study that may have been responsible for this outcome: 1) minute-by-minute validated air change rate measurements assuring good air

mixing in the test house, 2) elimination of confounding indoor sources, 3) more than 1400 measurements of time-varying variables (air change rate, indoor and outdoor concentrations) for 60 consecutive hours. These three strengths of the study may have contributed to the precision of the estimates. However, we note that precision is not accuracy. There could be bias from unknown causes affecting our results.

## References

- Jerrett, M.; Burnett, R.T.; Ma, R.; Pope, C.A.; Krewski, D.; Newbold, K.B.; Thurston, G.; Shi, Y.; Finkelstein, N.; Calle, E.E.; Thun, M.J. Spatial analysis of air pollution and mortality in Los Angeles, *Epidemiol.* 2005, 16, 727-736.
- Pope, C.A.; Burnett, R.T.; Thun, M.J.; Calle, E.E.; Krewski, D.; Ito, K.; Thurston, G.D. Lung cancer, cardiopulmonary mortality, and long-term exposure to fine particulate air pollution. *J. Am. Med. Assoc.* 2002, 287, 1132-1141.
- Stölzel, M.; Breitner, S.; Cyrys, J.; Pitz, M.; Wölke, G.; Kreyling, W.; Heinrich, J.; Wichmann, H.E.; Peters, A. Daily mortality and particulate matter in different size classes in Erfurt, Germany. *J. Expo. Sci. Environ. Epidemiol.* 2007, 458–467.
- Osunsanya, T.; Prescott, G.; Seaton, A. Acute respiratory effects of particles: mass or number? *Occup. Environ. Med.* 2001, 58, 154-159.
- Öberdorster, G.; Öberdorster, E.; Öberdorster, J. Nanotoxicology: An emerging discipline evolving from studies of ultrafine particles. *Environ. Health Persp.* 2005, 113, 823–839.
- Tran, C.L.; Buchanan, D.; Cullen, R.T.; Searl, A.; Jones, A.D.; Donaldson, K. Inhalation of poorly soluble particles: II Influences of particle surface area on clearance and inflammation. *Inhal. Toxicol.* 2000, 12,101–15.
- Utell, M.J.; Frampton, M.W.; Zareba, W.; Devlin, R.B.; Cascio, W.E. Cardiovascular effects associated with air pollution: Potential mechanisms and methods of testing. *Inhal. Toxicol.* 2002, 14, 1231-1247.
- Bräuner, E. V.; Forchhammer, L.; Møller, P.; Simonsen, J.; Glasius, M.; Wåhlin, P.; Raaschou-Nielsen, O.; Loft, S. Exposure to ultrafine particles from ambient air and oxidative stress-induced DNA damage. *Environ. Health Persp.* 2007, 115, 1177-82.
- Kittelson, D.B. Engines and nanoparticles: a review. *J. Aerosol Sci.* 1998, 29, 575-588.

- Seinfeld, J.H.; Pandis, S.N. *Atmospheric Chemistry and Physics*, 2nd, ed. Wiley: New York, 2006.
- Wallace, L.A.; Wang, F.; Howard-Reed, C.; Persily, A. Contribution of gas and electric stoves to residential ultrafine particle concentrations between 2nm and 64nm: Size distributions and emission and coagulation rates. *Environ. Sci. Technol.* 2008, 42, 8641–8647.
- He, C.R.; Morawska, L.D.; Hitchins, J.; Gilbert, D. Contribution from indoor sources to particle number and mass concentrations in residential houses. *Atmos. Environ.* 2004, 38, 3405-3415.
- Long, C.M.; Suh, H.H.; Catalano, P.J.; Koutrakis, P. Using time- and size-resolved particulate data to quantify indoor penetration and deposition behavior. *Environ. Sci. Technol.* 2001, 35, 2089–2099.
- Wallace, L.A. Ultrafine particles from a vented gas clothes dryer. *Atmos. Environ.* 2005, 39, 5777-5786.
- Szymczak, W.; Menzel, N.; Keck, L. Emission of ultrafine copper particles by universal motors controlled by phase angle. *J. Aerosol Sci.*, 2007, 38, 520-531.
- Coleman, B.K.; Destailats, H.; Hodgson, A.T.; Nazaroff, W.W. Ozone consumption and volatile byproduct formation from surface reactions with aircraft cabin materials and clothing fabrics. *Atmos. Environ.* 2008, 42, 642-654.
- Weschler, C.J. Ozone's impact on public health: Contributions from indoor exposures to ozone and products of ozone-initiated chemistry. *Environ. Health Persp.* 2006, 114, 1489-1496.
- Klepeis, N.E.; Nelson, W.C.; Ott, W.R.; Robinson, J.P.; Tsang, A.M.; Switzer, P.; Behar, J.V.; Hern, S.C.; Engelmann, W.H. The National Human Activity Pattern Survey (NHAPS): a resource for assessing exposure to environmental pollutants. *J. Expo. Anal. Environ. Epidemiol.* 2001, 11, 231-252.
- Tian, L.; Zhang, G.; Lin, Y.; Zhou, J.; Zhang, Q. Mathematical model of particle penetration through smooth/rough building envelop leakages. *Building Environ.* 2009, 44, 1144-1149.
- Liu, D. L.; Nazaroff, W. W. Modeling Pollutant Penetration Across Building Envelopes, *Atmos. Environ.* 2001, 35, 4451–4462.
- Thornburg, J.; Ensor, D.S.; Rodes, C.E.; Lawless, P.A.; Sparks, L.E.; Mosley, R.B. Penetration of particles into buildings and associated physical factors. part I: model development and computer simulations. *Aerosol Sci. Technol.* 2001, 34, 284–296
- Thatcher, T.L.; Lai, A.C.K.; Moreno-Jackson, R.; Sextro, R.G.; Nazaroff, W.W. Effects of room furnishings and air speed on particle deposition rates indoors. *Atmos. Environ.* 2002, 36, 1811-1819.

Vette, A.F.; Rea, A.W.; Lawless, P.A.; Rodes, C.E.; Evans, G.; Highsmith, V.R.; Sheldon, L. Characterization of indoor-outdoor aerosol concentration relationships during the Fresno PM exposure studies. *Aerosol Sci. Technol.* 2001, 34, 118–126.

Allen, R.; Wallace, L.; Larson, T.; Sheppard, L.; Liu, L.J.S. Evaluation of the recursive model approach for estimating particulate matter infiltration efficiencies using continuous light scattering data. *J. Expo. Sci. Environ. Epidemiol.* 2007, 17, 468-477.

Switzer, P.; Ott, W.R. Derivation of an indoor air averaging time model from the mass balance equation for the case of independent source inputs and fixed air exchange rates. *J. Expo. Anal. Environ. Epidemiol.* 1992, 2, 113-135.

Wallace, L.; Williams, R. Use of personal-indoor-outdoor sulfur concentrations to estimate the infiltration factor and outdoor exposure factor for individual homes and persons. *Environ. Sci. Technol.* 2005, 39, 1707–1714.

Hoek, G.; Kos, G.; Harrison, R.; de Hartog, J.; Meliefste, K. et al. Indoor–outdoor relationships of particle number and mass in four European cities. *Atmos. Environ.* 2008, 42: 156–169

Cyrus, J.; Pitz, M.; Bischof, W.; Wichmann, HE.; Heinrich, J. Relationship between indoor and outdoor levels of fine particle mass, particle number concentrations and black smoke under different ventilation conditions. *J. Expo. Anal. Environ. Epidemiol.* 2004, 14, 275-83.

*Standard test method for detecting air exchange in a single zone by means of a tracer gas dilution*; ASTM E741, American Society for Testing and Materials: Conshohocken, PA, 2000.

Howard-Reed, C.; Wallace, L.A.; Emmerich, S.J. Effect of ventilation systems and air filters on decay rates of particles produced by indoor sources in an occupied townhouse. *Atmos. Environ.* 2003, 37, 5295–5306

Lai, A.C.K.; Nazaroff, W.W. Modeling indoor particle deposition from turbulent flow onto smooth surfaces. *J. Aerosol Sci.* 2000, 31, 463-476.

De Levie, R. Estimating parameter precision in nonlinear least squares with Excel’s Solver, *J. Chem. Educ.* 1999, 76, 1594-1599.

De Levie, R. *Advanced Excel for Scientific Data Analysis*, Oxford University Press: New York, 2004.

Bennett, D.; Koutrakis, P., Determining the infiltration of outdoor particles in the indoor environment using a dynamic model. *J. Aerosol Sci.* 2006, 37, 766-785

Hinds, W.C. *Aerosol Technology: Properties, Behavior, and Measurement of Airborne Particles*, 2<sup>nd</sup>, ed. Wiley: New York, 1999.

Zhu, Y.; Hinds, W.C.; Krudysz, M., Kuhn, T.; Fronies, J.; Sioutas, C. Penetration of freeway ultrafine particles into indoor environments. *J. Aerosol Sci.* 2005, 36, 303–322.

Chao, C.Y.H.; Wan, M.P.; Cheng, E.C.K. Penetration coefficient and deposition rate as a function of particle size in non-smoking naturally ventilated residences. *Atmos. Environ.* 2003, 37, 4233–4241.

Wallace, L.A.; Emmerich, S.J., Howard-Reed, C. Effect of central fans and in-duct filters on deposition rates of ultrafine and fine particles in an occupied townhouse, *Atmos. Environ.* 2004, 38, 405-413.

**Acknowledgements.** Daniel Greb and Steven Nabinger operated the NIST test house tracer gas analyzer and environmental monitoring devices. We thank William W. Nazaroff of the University of California Berkeley for supplying the spreadsheet used to calculate deposition rates in the Lai-Nazaroff model. We also thank four anonymous reviewers for their valuable comments.

### **Supporting Information Available**

A schematic diagram of the manufactured test house, further details regarding quality assurance for the measurement methods, and examples of time-varying air change rate and UFP concentrations are shown. The effect of choosing the sum of absolute errors rather than the sum of the squares of the errors to minimize in determining the parameters  $P$ ,  $k_{comp}$ , and  $F_{inf}$  is also shown.

## Figure captions

Figure 1. Observed and modeled UFP concentrations for 22 nm to 26 nm particles

Figure 2. Regression between observed and modeled concentrations

Figure 3. Size-resolved UFP infiltration factors a) for closed windows (9 weekend measurements) and b) for the case of one window open 7-8 cm (10 weekend measurements)

Figure 4. a) Particle penetration coefficients observed with open and closed windows. b) Composite deposition rate  $k_{comp}$  for open and closed window. Error bars are standard errors.

Figure 1

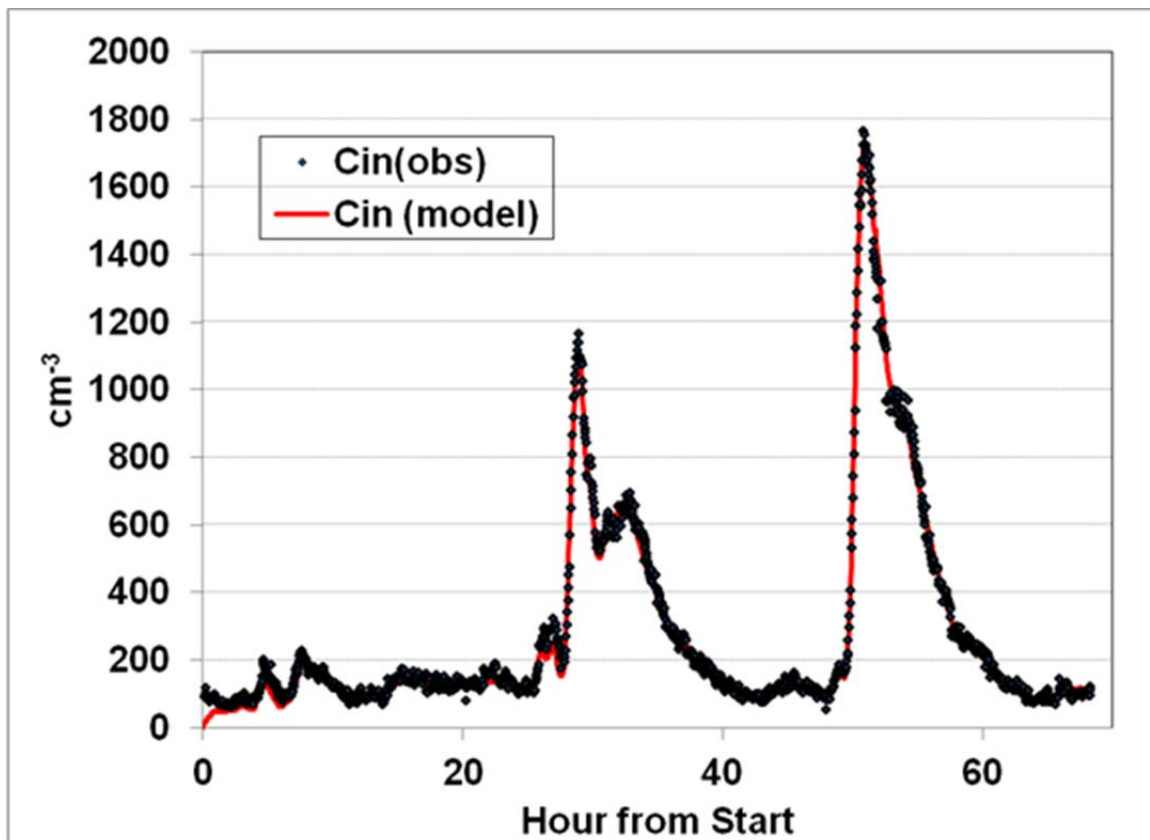


Figure 2

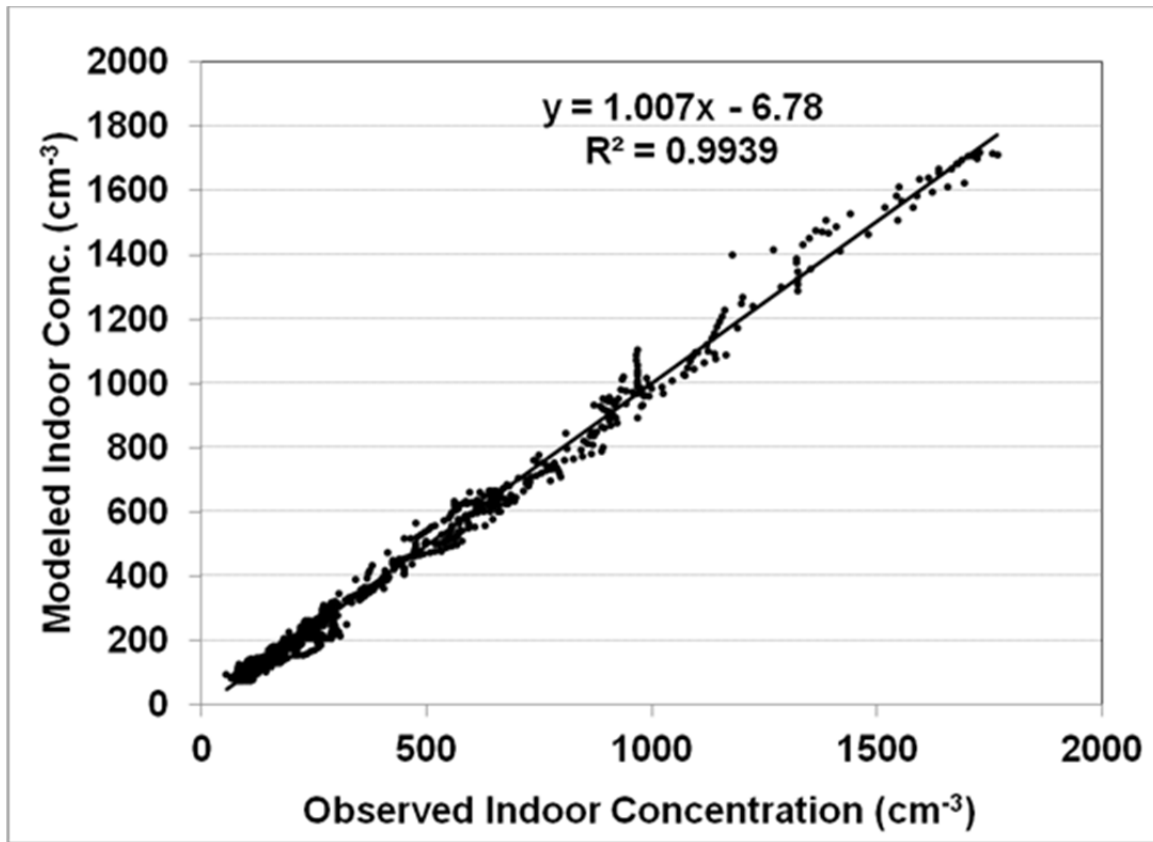
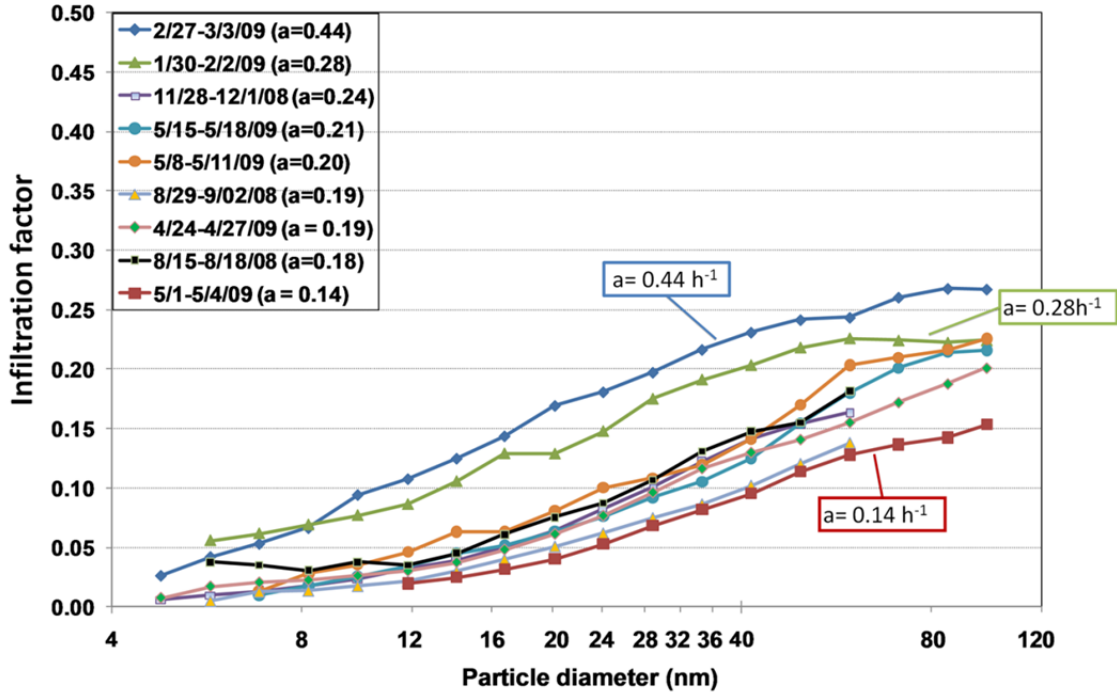


Figure 3

(a) Closed Window



(b) Open window

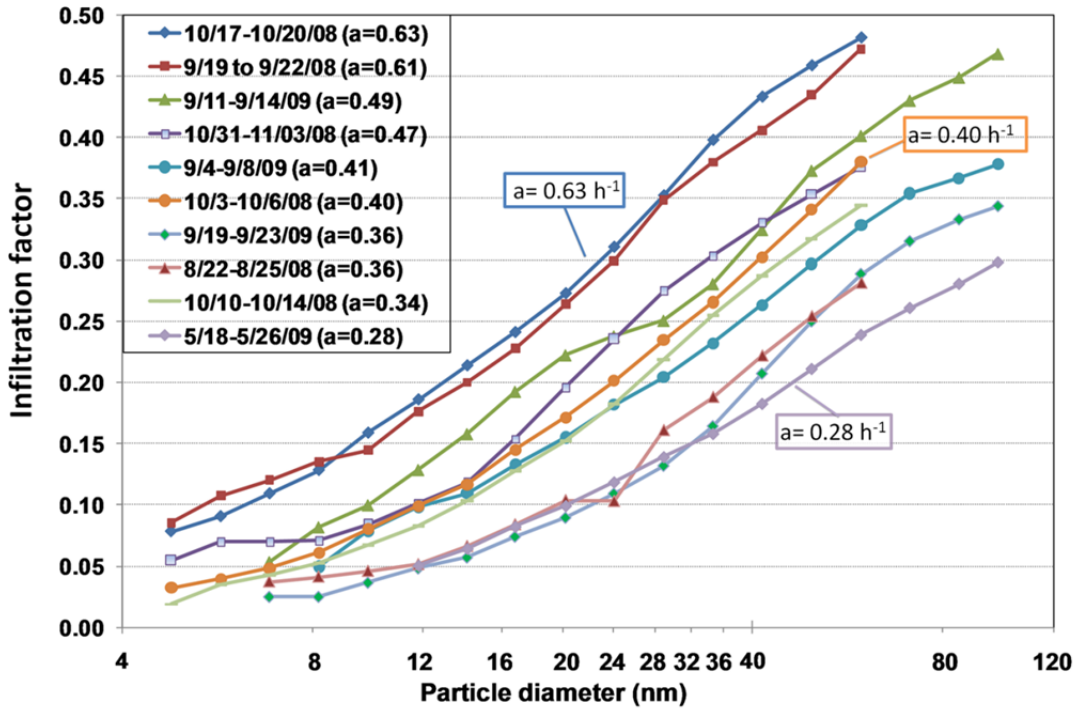
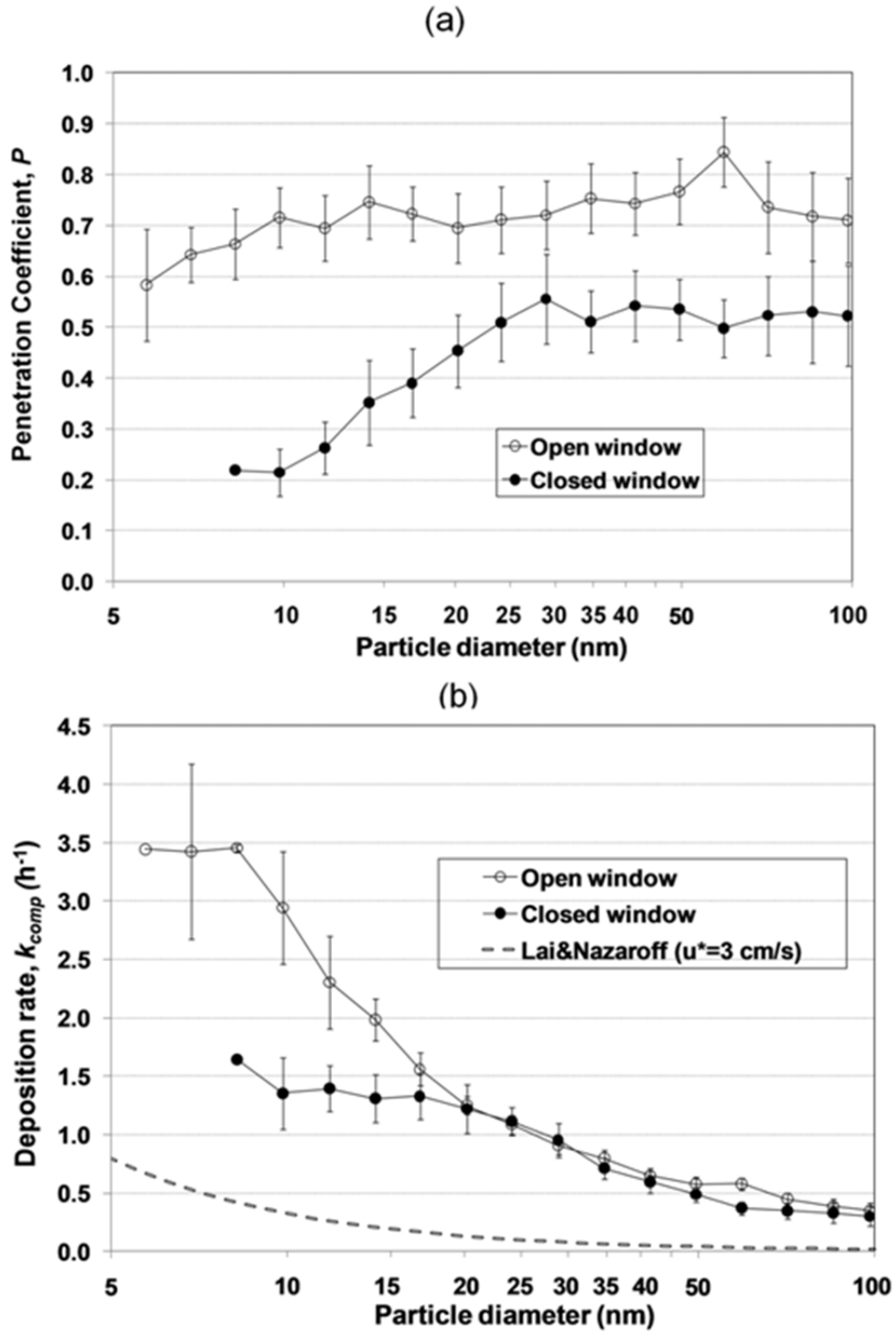


Figure 4



**Table 1. Percent Uncertainties (Standard Errors) in Estimates of  $P$ ,  $k$ , and  $F_{inf}$  for two example cases.**

<b>Closed Windows (4/24 to 4/27/09)</b>				<b>Open Window (10/17 to 10/20/08)</b>			
<b>Diam. (nm)</b>	<b><math>P</math></b>	<b><math>k</math></b>	<b><math>F_{inf}</math></b>	<b>Diam. (nm)</b>	<b><math>P</math></b>	<b><math>k</math></b>	<b><math>F_{inf}</math></b>
7.6-8.8	2.4	3.0	3.9	5.3-6.2	4.1	5.0	6.5
9-11	1.7	2.2	2.8	6.4-7.4	2.6	3.2	4.1
11-13	1.3	1.6	2.1	7.6-8.8	2.3	2.8	3.6
13-15	1.3	1.6	2.0	9-11	1.8	2.2	2.9
16-18	0.9	1.1	1.4	11-13	1.7	2.2	2.8
19-22	0.7	1.0	1.2	13-15	1.6	2.1	2.6
22-26	0.7	0.9	1.2	16-18	1.3	1.8	2.2
27-31	0.6	0.9	1.1	19-22	0.9	1.4	1.7
32-37	0.7	1.1	1.3	22-26	0.6	1.0	1.1
38-44	0.4	0.6	0.8	27-31	0.6	1.0	1.2
46-53	1.5	2.0	2.5	32-37	0.8	1.4	1.6
55-64	1.0	1.4	1.7	38-44	1.3	2.3	2.7
66-76	0.7	1.0	1.2	46-53	1.8	3.3	3.8
79-91	0.6	0.8	1.0	55-64	2.1	3.7	4.3
95-106	0.7	1.1	1.3				
<b>Mean</b>	<b>1.0</b>	<b>1.4</b>	<b>1.7</b>		<b>1.7</b>	<b>2.4</b>	<b>2.9</b>
<b>SD</b>	<b>0.5</b>	<b>0.6</b>	<b>0.8</b>		<b>0.9</b>	<b>1.1</b>	<b>1.4</b>

**Table 2.  $F_{inf}$  estimates vs. ratios of mean indoor and outdoor concentrations  $C_{in}/C_{out}$**

Particle diameter (nm)	Closed Window		Open Window	
	$F_{inf}$	$C_{in}/C_{out}$	$F_{inf}$	$C_{in}/C_{out}$
<b>4.4-5.1</b>			<b>0.08</b>	<b>0.09</b>
<b>5.3-6.2</b>			<b>0.09</b>	<b>0.11</b>
<b>6.4-7.4</b>			<b>0.11</b>	<b>0.12</b>
<b>7.6-8.8</b>			<b>0.13</b>	<b>0.14</b>
<b>9-11</b>	<b>0.03</b>	<b>0.03</b>	<b>0.15</b>	<b>0.17</b>
<b>11-13</b>	<b>0.03</b>	<b>0.04</b>	<b>0.18</b>	<b>0.20</b>
<b>13-15</b>	<b>0.04</b>	<b>0.05</b>	<b>0.21</b>	<b>0.23</b>
<b>16-18</b>	<b>0.05</b>	<b>0.06</b>	<b>0.24</b>	<b>0.26</b>
<b>19-22</b>	<b>0.06</b>	<b>0.07</b>	<b>0.27</b>	<b>0.29</b>
<b>22-26</b>	<b>0.08</b>	<b>0.09</b>	<b>0.31</b>	<b>0.32</b>
<b>27-31</b>	<b>0.10</b>	<b>0.11</b>	<b>0.35</b>	<b>0.35</b>
<b>32-37</b>	<b>0.12</b>	<b>0.13</b>	<b>0.40</b>	<b>0.39</b>
<b>38-44</b>	<b>0.13</b>	<b>0.16</b>	<b>0.43</b>	<b>0.42</b>
<b>46-53</b>	<b>0.14</b>	<b>0.16</b>	<b>0.45</b>	<b>0.43</b>
<b>55-64</b>	<b>0.16</b>	<b>0.17</b>	<b>0.47</b>	<b>0.45</b>
<b>66-76</b>	<b>0.17</b>	<b>0.18</b>		
<b>79-91</b>	<b>0.19</b>	<b>0.19</b>		
<b>95-106</b>	<b>0.20</b>	<b>0.20</b>		

## SUPPORTING INFORMATION

### Quality control

This study focused on the contribution of particles of outdoor origin to the indoor UFP concentrations; indoor activities were avoided by conducting the measurements in an unoccupied house during weekends. Measurements of air change rate and indoor-outdoor UFP concentrations normally occurred between late afternoon Friday and Monday morning. During the decay test, the tracer gas was injected every 4 hours and the tracer gas concentration in each room was measured sequentially each minute, completing a cycle in 10 minutes. Following the injection of the tracer gas, about one hour was allowed for complete mixing to be achieved, and the air change rates were calculated using regression analysis. The regressions were performed as a running one-hour average every 10 minutes.

The mean and standard deviation of the air change rates for the six monitoring locations were calculated. Given that air mixing might be imperfect and the air change rate varies spatially within the house, the relative standard deviation (RSD) of the SF<sub>6</sub> concentrations and the associated air exchange rates over the previous hour were calculated for every 10-minute interval. The RSD values provided information on incomplete mixing of tracer gas. Periods with high RSDs (> 10%) that occurred during the initial decay period indicated incomplete mixing of the tracer gas and were excluded in the analysis of air change rate. Also, in later time periods of the decay, if high RSDs lasted more than 10 minutes, the data were not used in the analysis. The majority of the data had RSDs <10%.

To calculate the uncertainty of the air change rate, the relative standard error (RSE) of the regression slope was determined for each of the six rooms. This error includes both the uncertainty due to incomplete mixing across rooms and the precision (repeatability of the measurement of the same concentration). The average ( $\pm$ SD) of the RSE values was  $6.5 \pm 1.4$  % for the cases with closed windows and  $4.3 \pm 5.9$  % for the cases with one window open.

The tracer gas analyzer was calibrated every week against known concentrations ranging from 5 ppb to 150 ppb (18 point calibration) with the limit of detection of 5 ppb. The calibration parameters of the monitoring instrument (GC/ECD) might drift between successive calibrations. Therefore, the error due to electronic drift of the instrument was analyzed by observing the variation of calibration slope and intercept for successive calibrations. Most of the errors due to the calibration drift were less than 5 %, and the maximum error was 13 %.

The two measurement uncertainties, denoting 1) the uncertainty due to incomplete air mixing plus precision (4.3% to 6.5%) and 2) the uncertainty due to drift of the instrument (5 %), are independent. Therefore, adding the two uncertainties in quadrature gives the total error for the estimation of air change rate of approximately 8% with a maximum of 15 %.

Indoor and outdoor UFP samples were collected at a height of 1.5 m above the floor and ground. Particle deposition occurred in the sampling tubes and the particle losses in the sampling tubes were calculated. The lengths of the indoor and outdoor sampling tubes were roughly the same (~ 50 cm), and even though the indoor sampling tube had a bend of approximately 130°, the difference in particle loss between sampling the two tubes was measured as less than 7 %. Usually four consecutive samples were collected in each microenvironment. Because the change from one environment to the other might temporarily affect the instrument response, the first sample was visually compared to the following three and was not included in the calculations if it was distinctly different.

For the accuracy of measurements of particle size and concentration, no reference calibration procedure exists. However, the key factors affecting the particle measurement data were checked as the following:

- 1) DMA voltage – The reliable high voltage scheme was required for the electrical mobility analyzer. The DMA voltages were annually calibrated with NIST traceable meters.

2) CPC and DMA airflow –It was extremely important to ensure that inlet sheath flow was accurate and laminar in the DMA, and precisely matches the exhaust flow. As small flow disturbances could result in decreased resolution, aerosol flow rates were measured before and after each experiment using a bubble flow rate meter. At least three measurements were taken and all three were required to be within 2% of the desired rate.

3) Scan time – the duration of the scan affects the accuracy of the measurement. Scan time effect, which causes a tail toward large particle sizes resulting from turbulent mixing in the plumbing between DMA and CPC, could occur during short scans (TSI, 2008). In the present study, 150 seconds of scan time was used and this provided enough accuracy for the analysis of the 2 nm to 100 nm particles.

4) Bipolar charge distribution – The measurement accuracy for the size distribution and concentration depends on the charge distribution of the incoming aerosol. The SMPS uses a radioactive ionizer (the beta-emitter Krypton-85) to induce a bi-polar charge distribution. In this study, a stronger radiation source (3080N electrostatic classifier, TSI, Shoreview, MN) was used to improve the charging efficiency for the smallest particles.

5) Efficiency curve of the CPC – Based on the measurement efficiency curve for CPC, the correct particle size distribution is built. The minimum measurable particle size, defined as cut-off size, is the size at which the CPC can detect 50 % of the particles. The cut-off size depends on the efficiency of the optical system and hygroscopic property of particles. For water-soluble inorganic particles the cut-off size ranges from 3 nm to 5 nm whereas it is larger than 8 nm for hydrophobic organic particles. Due to the higher cut-off size for water-insoluble particles, the measurement of particles smaller than 8 nm should be interpreted with caution.

6) DMA transfer function – Based on the ratio of sheath flow to aerosol sampling flow, the width of the particle size distribution is determined. For optimal performance, a sheath to aerosol ratio of 10:1 was used. With this ratio, each particle size bin totally represents the size data at each voltage.

7) Diffusion loss –The particle loss due to diffusion has significant effects on monitoring nanoparticles since the largest force acting on nanoparticles is diffusion. Internal particle losses due to diffusion were reduced as much as possible by using minimal tubing and removing the impactor from the nozzle inlet. Also, a manufacturer-supplied diffusion correction based on the estimated losses to internal instrument pathways was applied to all the data.

### **Temporal air change rate and UFP concentration**

Figure S2 presents an air change rate profile measured during three days in August 2008. Figure S2 shows that air change rate fluctuates between  $0.1 \text{ h}^{-1}$  and  $0.3 \text{ h}^{-1}$  likely due to variations in the indoor-outdoor temperature difference and wind speed. Figure S3 shows ultrafine concentration profiles for indoors (red dots) and outdoors (black dots) that were monitored for the corresponding three days in August 2008. Indoor concentrations are consistently lower than the outdoor concentrations due to penetration and deposition losses, and the indoor profile tracks the outdoor profile with a time lag. The peak outdoor particle concentrations were observed during the daytime and this trend may be explained by presence of strong UFP emission sources during the daytime period such as increased traffic density or atmospheric nucleation bursts.

### **Uncertainty of estimates of $P$ , $k_{comp}$ , and $F_{inf}$ .**

The use of a formal algorithm to calculate the uncertainty of the estimates of  $P$  and  $k_{comp}$  is discussed in the main text. Since the program assumes minimization of the sum of squared errors, whereas our initial approach chose minimization of the sum of absolute differences between observed and predicted values, we recalculated the estimates of  $P$  and  $k_{comp}$  using the sum of squared errors for two sets of measurements including both a closed window and open window case. The resulting differences in the estimates of  $P$ ,  $k_{comp}$ ,  $F_{inf}$ , and  $R^2$  are provided in Tables S1 and S2.

A third approach was to consider the effect on the sum of errors of a 10% change in  $P$  or  $k_{comp}$ . A change in one without a change in the other typically caused a change in the sum of errors ranging between 10

and 20%. This suggested that the solution surface was quite steep when going “across” rather than longitudinally down the “valley” representing the best estimate of the infiltration factor. Therefore a 10% change was imposed on one parameter, the corresponding change in the other parameter in order to keep the infiltration factor constant was also imposed, and the change in the sum of squares was noted. These approaches were tried on 7 cases. Generally, a 10% change in  $k_{comp}$  caused a range of changes in  $P$  of similar magnitude, but only a 0.46% to 8% increase in the sum of squared errors. Although this appears to be a small increase, even the smallest value of 0.46% is about two orders of magnitude larger than the Solver Aid estimates of the standard errors, which never exceeded 0.004%. Therefore, even this small increase in the sum of squared errors is well outside the range of the estimated uncertainty.

### **Comparison of Estimates with Theory**

Theoretical and experimental studies of penetration have been carried out by Liu and Nazaroff (31). Their study assumes smooth rectangular cracks and finds a dependence of the penetration coefficient on the length and height of the crack, the indoor-outdoor pressure difference, and particle size. For ultrafine particles, the theory predicts an increase in the penetration coefficient with increasing particle diameter until a maximum is reached. The maximum varies from 1 downward depending on the four parameters mentioned above. Our results for the closed window case show an increase with increasing size for the smaller ultrafines, and a relatively low maximum value near 0.6. This corresponds in general terms to their results but the match to the theoretical shape of the curve is not satisfactory. A possible explanation for this discrepancy is non-uniform crack height and crack flow length in the real building. The experimental data were collected for the rough and irregular cracks of unknown shape, length, and height in a real building, whereas the model predictions assumed a smooth rectangular channel.

Theoretical studies of deposition have been carried out by Lai and Nazaroff (31). Their studies predict an increase in deposition rate for the smaller UFP. Our results show a similar increase. However, since our experiments included not only deposition to building surfaces but also deposition in duct work and on the

furnace filter due to the forced-air central fan, our results greatly exceed the theoretical estimates for surface deposition only. The air recirculation rate due to the fan was  $4.95 \text{ h}^{-1}$ , more than 10 times larger than the average outdoor air change rate. This high recirculation rate implies that significant particle removal due to filtration in the central HVAC system and deposition in ductwork likely occurred. In this study, the HVAC filter had been operating more than 2 years and the Minimum Efficient Reporting Value (MERV) of the filter was low ( $< 3$ ). However, the filter efficiency for UFP is very high ( $> 90 \%$ ) and expected to increase as particle size decreases down to 5 nm. In addition, the surface roughness associated with the carpeted floor surface might increase the friction velocity, causing higher particle removal rate than predicted (31).

**Figure captions**

Figure S1. Floor plan of the manufactured test house located at NIST (Gaithersburg, MD)

Figure S2. Air change rates during one weekend.

Figure S3. UFP concentrations indoors and outdoors during one weekend

Figure S1

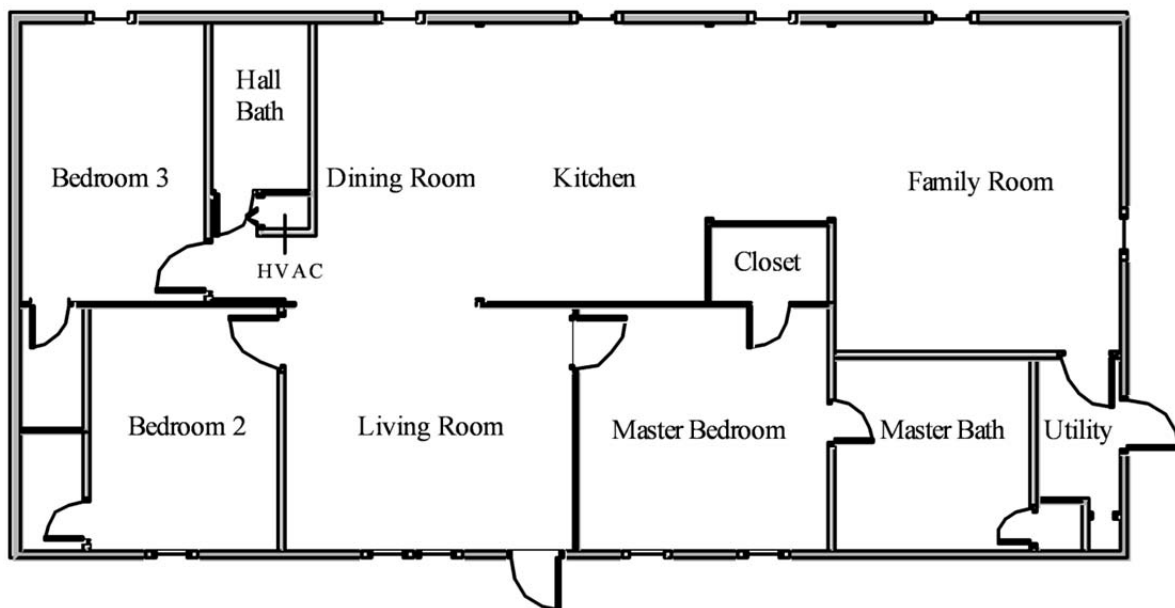


Figure S2

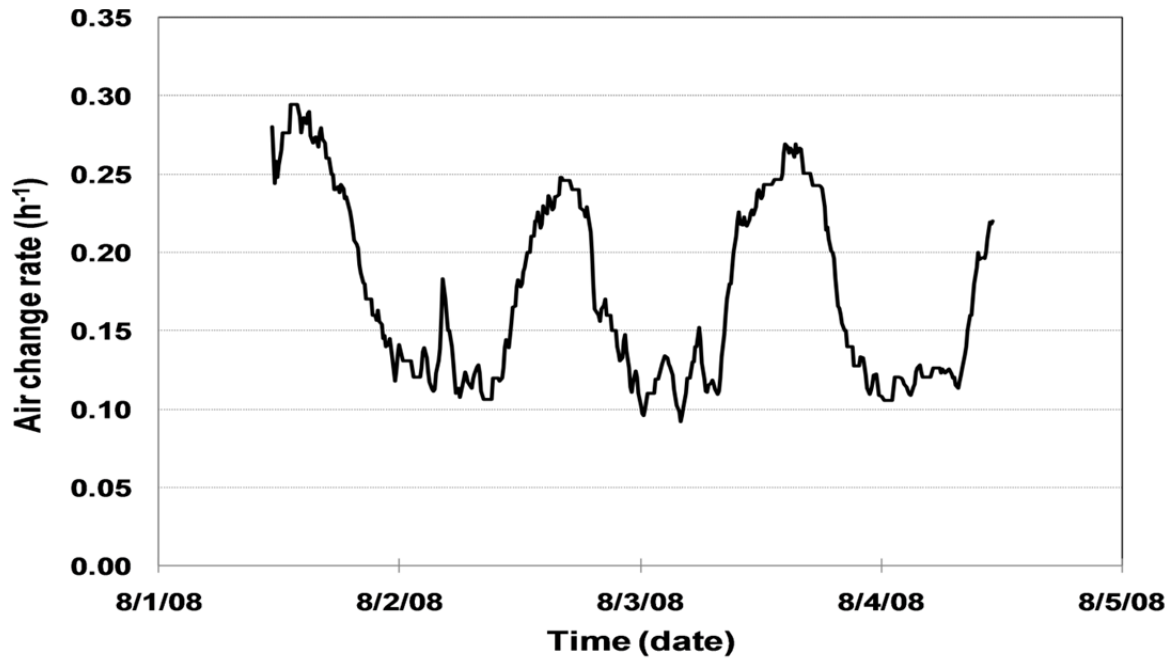


Figure S3

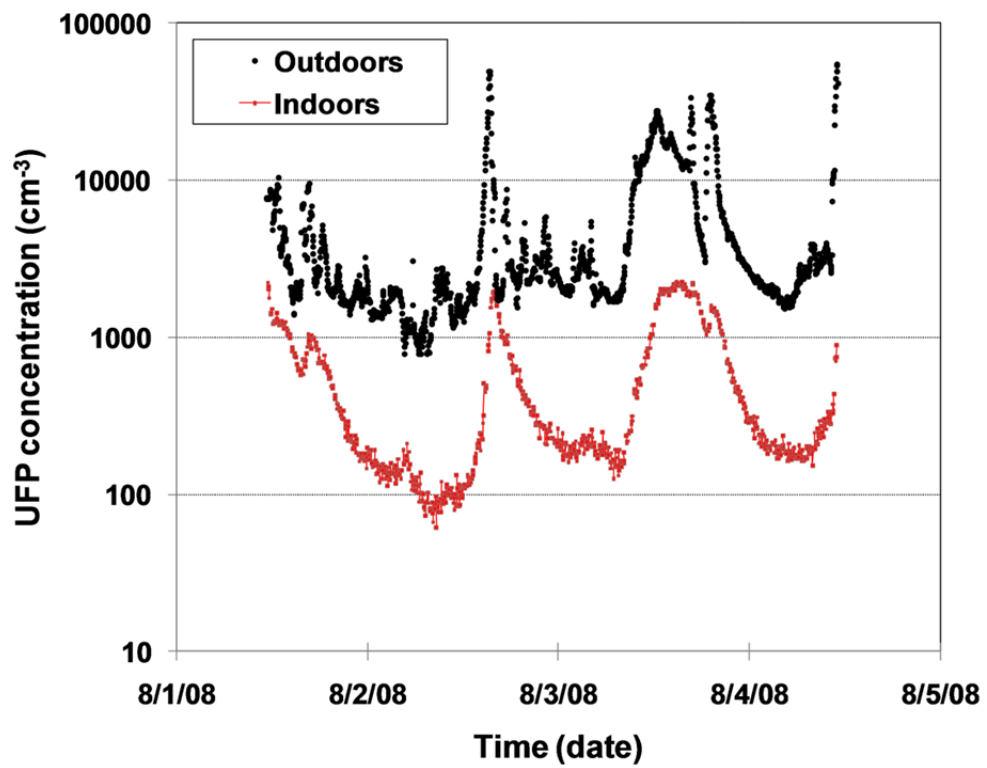


Table S1. Percent Differences in Parameter Estimates Due to Minimizing the Sum of Squared Errors vs the Sum of Absolute Differences

Closed Window Case: Data from 4/24 to 4/27/09 (N=1648 measurements over 68.7 hours)

Range of diameters (nm)	Penetration coefficient $P$			Deposition rate $k_{comp}$ ( $h^{-1}$ )			$R^2$			Infiltration Factor $F_{inf}$		
	Squared errors	Absolute errors	% diff	Squared errors	Absolute errors	% diff	Squared errors	Absolute errors	% diff	Squared errors	Absolute errors	% diff
7.6-8.8	0.206	0.219	-6.1	1.453	1.644	-11.6	0.836	0.824	1.5	0.024	0.022	4.7
9-11	0.271	0.267	1.5	1.740	1.740	0.0	0.929	0.909	2.2	0.026	0.026	1.4
11-13	0.285	0.287	-0.5	1.501	1.597	-6.0	0.959	0.952	0.7	0.032	0.030	5.1
13-15	0.321	0.327	-1.6	1.332	1.450	-8.1	0.958	0.953	0.5	0.040	0.037	5.9
16-18	0.395	0.389	1.4	1.335	1.330	0.4	0.979	0.980	-0.1	0.049	0.048	1.0
19-22	0.421	0.425	-0.9	1.069	1.116	-4.2	0.985	0.982	0.3	0.063	0.061	2.7
22-26	0.475	0.477	-0.4	0.941	0.979	-3.8	0.985	0.987	-0.2	0.079	0.077	2.9
27-31	0.522	0.529	-1.2	0.811	0.844	-3.9	0.988	0.987	0.1	0.098	0.096	1.9
32-37	0.601	0.605	-0.8	0.750	0.789	-4.9	0.974	0.973	0.1	0.120	0.117	3.2
38-44	0.707	0.706	0.2	0.759	0.832	-8.8	0.903	0.908	-0.6	0.140	0.130	7.9
46-53	0.735	0.668	9.9	0.750	0.703	6.6	0.869	0.867	0.2	0.147	0.141	4.4
55-64	0.650	0.637	2.1	0.596	0.583	2.3	0.931	0.928	0.3	0.156	0.155	0.3
66-76	0.638	0.628	1.7	0.515	0.497	3.5	0.959	0.953	0.6	0.171	0.172	-0.9
79-91	0.704	0.718	-2.0	0.520	0.531	-2.0	0.965	0.958	0.7	0.187	0.188	-0.5
95-106	0.759	0.763	-0.5	0.522	0.524	-0.4	0.942	0.933	1.0	0.201	0.201	-0.2
Mean			2.1			4.4			0.6			2.9
SD			2.6			3.3			0.6			2.3

Table S2. Percent Differences in Parameter Estimates Due to Minimizing the Sum of Squared Errors vs the Sum of Absolute Differences

Open Window Case: Data from 10/27 to 10/30/08 (N = 1648 measurements over 68.7 hours)

Range of diameters (nm)	Penetration coefficient $P$			Deposition rate $k_{comp}$ ( $h^{-1}$ )			$R^2$			Infiltration Factor $F_{inf}$		
	Squared errors	Absolute errors	% diff	Squared errors	Absolute errors	% diff	Squared errors	Absolute errors	% diff	Squared errors	Absolute errors	% diff
5.3-6.2	0.700	0.694	0.9	4.085	4.195	-2.6	0.928	0.920	0.9	0.093	0.090	2.6
6.4-7.4	0.739	0.698	5.9	3.619	3.394	6.7	0.954	0.950	0.4	0.109	0.109	-0.3
7.6-8.8	0.762	0.724	5.1	3.047	2.927	4.1	0.966	0.964	0.2	0.130	0.128	1.1
9-11	0.829	0.792	4.6	2.742	2.513	9.1	0.974	0.972	0.2	0.154	0.159	-3.0
11-13	0.905	0.890	1.7	2.473	2.384	3.7	0.978	0.976	0.2	0.183	0.186	-1.7
13-15	0.888	0.875	1.5	1.993	1.950	2.2	0.978	0.978	0.0	0.212	0.214	-0.7
16-18	0.879	0.867	1.3	1.662	1.638	1.4	0.982	0.982	0.0	0.240	0.241	-0.2
19-22	0.859	0.844	1.7	1.357	1.321	2.7	0.987	0.986	0.1	0.271	0.272	-0.6
22-26	0.823	0.826	-0.3	1.053	1.046	0.7	0.994	0.993	0.1	0.307	0.310	-1.2
27-31	0.825	0.825	0.0	0.848	0.845	0.3	0.992	0.991	0.1	0.350	0.352	-0.6
32-37	0.897	0.886	1.3	0.782	0.772	1.3	0.988	0.986	0.2	0.399	0.398	0.3
38-44	0.978	0.947	3.3	0.795	0.747	6.3	0.967	0.966	0.1	0.431	0.433	-0.5
46-53	0.970	0.966	0.5	0.726	0.696	4.3	0.957	0.953	0.4	0.449	0.459	-2.1
55-64	1.019	1.028	-0.8	0.735	0.715	2.8	0.974	0.971	0.3	0.469	0.481	-2.6
Mean			2.1			3.4			0.2			1.3
SD			1.9			2.5			0.2			1.0